International Journal of Concrete Structures and Materials
Vol.6, No.1, pp.31~40, March 2012
DOI 10.1007/s40069-012-0003-2
ISSN 1976-0485 / eISSN 2234-1315

Development and Applications of the Intrinsic Model for Formwork Pressure of Self-Consolidating Concrete

Seung Hee Kwon,[1)] Jae Hong Kim,[2),*] and Surendra P. Shah[3)]

(Received October 5, 2011, Revised February 16, 2012, Accepted February 16, 2012)

Abstract: Self-consolidating concrete (SCC) is a recently developed innovative construction material. SCC fills in a formwork without any vibrating consolidation, which allows us to eventually achieve robust casting. However, high formwork lateral pressure exerted by SCC is a critical issue regarding its application as cast-in-place concrete. In order to control the risk caused by high formwork pressure, a comprehensive prediction model for the pressure was previously proposed, investigated, and validated with various SCC mixtures. The model was originally designed to simulate the intrinsic pressure response of SCC mixtures while excluding other extrinsic influencing factors such as friction and flexibility of the formwork. The model was then extended to consider extrinsic factors such as friction between SCC mixtures and formwork. In addition, other interesting topics for peak formwork pressure and mineral admixture effects were summarized in the paper.

Keywords: Formwork, SCC, prediction model, peak pressure, friction, mineral admixture.

1. Introduction

Self-consolidating concrete (SCC) has been well established in the precast concrete industry, and currently much effort is being exerted to apply SCC to cast-in-place.[1,2] There are some challenges in using SCC in cast-in-place. One of the major obstacles is high formwork lateral pressure. Formwork pressure of SCC is much higher than that of ordinary concrete due to its high fluidity. Practitioners experience significant difficulty in designing formwork for SCC, including determining the placement rate and the removal time of formwork. This provides motivation to accurately predict the formwork pressure exerted by SCC and to find a way to reduce the formwork pressure.

The Center for Advanced Cement-Based Materials (ACBM) has been carrying out extensive studies related to formwork pressure of SCC. A technique for experimental simulation was developed[3] that allows observation of the behavior of SCC formwork pressure. The various notable findings include that the pressure response of SCC mixtures shows thixotropy in a similar manner to its rheological behavior. Therefore, the model considers two different situations of thixotropic SCC mixtures, one under increasing pressure and the other under sustained constant pressure.

Prior to describing the model, it is necessary to categorize influencing factors on formwork pressure. There are many factors affecting formwork lateral pressure such as placement rate, mixture consistency, mix proportion, temperature, form smoothness, dimension and shape of the form, consolidation method, type and contents of admixture, content and type of cement, the height of concrete placement, and viscosity and yield stress of concrete. Some factors are related to the intrinsic characteristics of the material itself while others are extrinsic factors related to external conditions. A prediction model only for the intrinsic characteristics was first developed.[4] Subsequently, the extrinsic were separately incorporated into the intrinsic model.[5] Although the model was motivated by the need to predict the formwork pressure of SCC, it can also be applied to any cement-based materials, including cement paste, mortar, and ordinary concrete. The intrinsic model is capable of predicting the whole evolution of the pressure from the beginning of casting to cancellation of the pressure. In order to predict the peak pressure, a simple analytical model was also suggested through modification of the original intrinsic model[6]. In addition to the work on prediction, the effects of admixtures on formwork pressure were investigated to seek a way to reduce the peak pressure.[7]

This paper reviews and introduces recent works on SCC formwork pressure. The series of studies performed in the Center for ACBM are explained, and finally research that needs to be performed in the near future is recommended.

2. Model development

2.1 Proposition of the intrinsic model

Overhead or vertical pressure can be employed as a parameter

[1)]Department of Civil and Environmental Engineering, Myongji University, Gyeonggi 449-728, Korea.
[2)]School of Urban and Environmental Engineering, Ulsan National Institute of Science and Technology (UNIST), Ulsan 689-798, Korea.
*Corresponding Author; E-mail: jaekim@unist.ac.kr
[3)]Center for Advanced Cement-Based Materials, Northwestern University, Evanston, IL, 60208, USA.

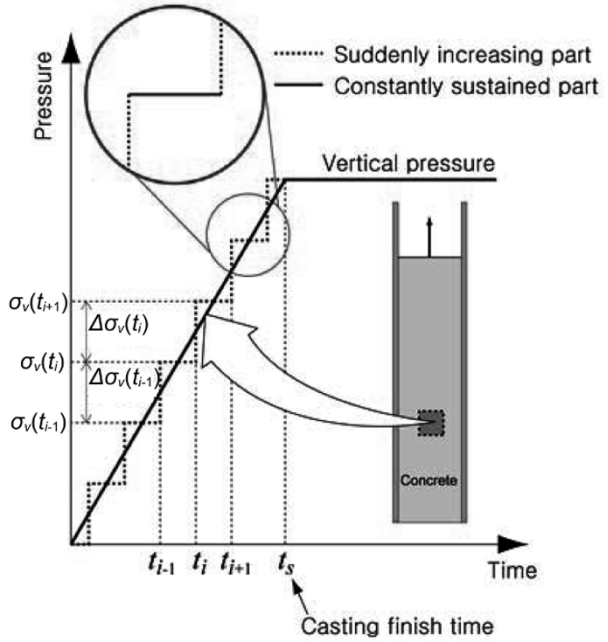

Fig. 1 Consideration of overhead pressure as stepwise loading (redrawn from Kwon et al.[4]).

to idealize the situation of concrete casting. The vertical pressure increases up to the end of casting, and is then constantly sustained. In a similar manner, the continuous increase of overhead pressure could be discretized as a stepwise loading, as shown in Figure 1. The stepwise loading consists of two parts: a sudden increase followed by a constant load.

The intrinsic model[4] assuming thixotropic behavior for formwork pressure separates the lateral pressure responses according to the sudden increase vs. the constant sustaining of the vertical pressure. The instantaneous function $\beta(t)$ is a response to the suddenly applied vertical pressure, defined as the ratio of lateral-to-vertical pressure applied at time t. The delayed function $\alpha(t, t')$ is defined as the ratio of the lateral pressure change for time duration $(t\text{-}t')$ exerted by the vertical pressure applied at time t', and therefore it represents the gradual decrease of the lateral pressure under the constantly sustained vertical pressure. The two functions are expressed as follows:

$$\beta(t) = \begin{cases} 1 - s_1 t & for\ t \le t_b \\ \beta_b - s_2(t - t_b) & for\ t > t_b \end{cases} \text{ and} \tag{1}$$

$$\alpha(t,t') = \begin{cases} 1 - U_{pc}\left(\dfrac{t-t'}{t_c-t'}\right)^n & for\ t \le t_c \\ U_{pc} + \dfrac{t-t_c}{t_e-t_c}\alpha(t,t') & for\ t > t_c \end{cases} \tag{2}$$

In Eq. (1), t_b is the time at which the slope of $\beta(t)$ is changed, β_s is the value of $\beta(t)$ at time t_b, and s_1 and s_2 are the initial slope and the slope after t_b, respectively. In Eq. (2), t' is the time when vertical pressure is applied, t_e is the dissipation time of the lateral pressure, t_c is the time when the rate of decrease of $\alpha(t, t')$ is suddenly changed, U_{pc} is the value of $\alpha(t, t')$ at $t' = t_c$, and n is an exponent representing the nonlinearity of the initial part of $\alpha(t, t')$. Figure 2 graphically depicts the two functions.

Under the assumption that $\beta(t)$ and $\alpha(t, t')$ for a given cement-based material are independent of the applied vertical pressure, the lateral pressure can be calculated with a linear superposition.[4] The lateral pressure consequently becomes cumulative pressure response to the applied vertical pressure:

$$\sigma_L(t) = \int_0^t \alpha(t,t')\beta(t')d\sigma_V(t') \tag{3}$$

where $\sigma_L(t)$ is the lateral pressure at an arbitrary time t and is expressed as the sum of the response to $d\sigma_V(t')$, each increment of the vertical pressure applied at time $t' < t$. Figure 3 describes the calculation method for an incremental vertical pressure.

2.2 Experimental verification of the model

A special apparatus was manufactured to measure the lateral pressure excluding the effects of extrinsic factors such as formwork friction and deformation, as presented in Figure 4. Two pressure cells of 175 kPa (20 psi) capacity were attached at the middle of both sides, and one additional cell was located at the bottom to confirm that there is no effect of wall friction.

Experiments were performed with cement paste (CP), ordinary concrete (OC), and SCC, the mix proportions of which are shown

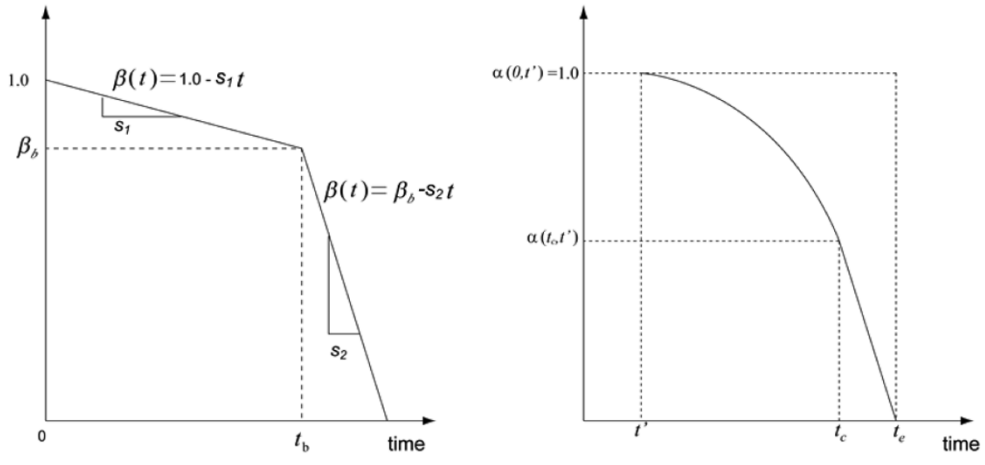

(a) function $\beta(t)$ **(b) function $\alpha(t,t')$**

Fig. 2 Graphical description of two functions (redrawn from Kwon et al.[4]).

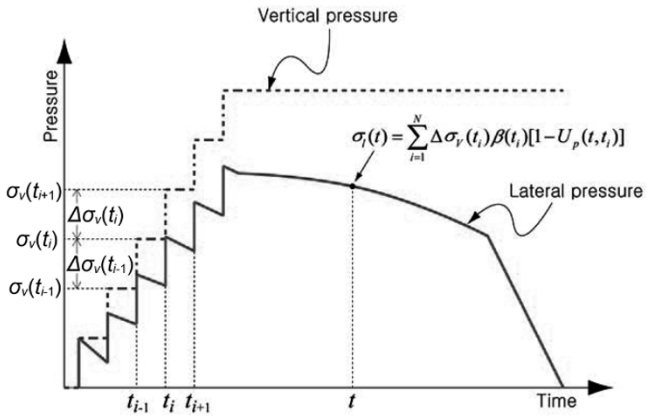

Fig. 3 Calculation of lateral pressure for stepwise variation of vertical pressure (redrawn from Kwon et al.[4]).

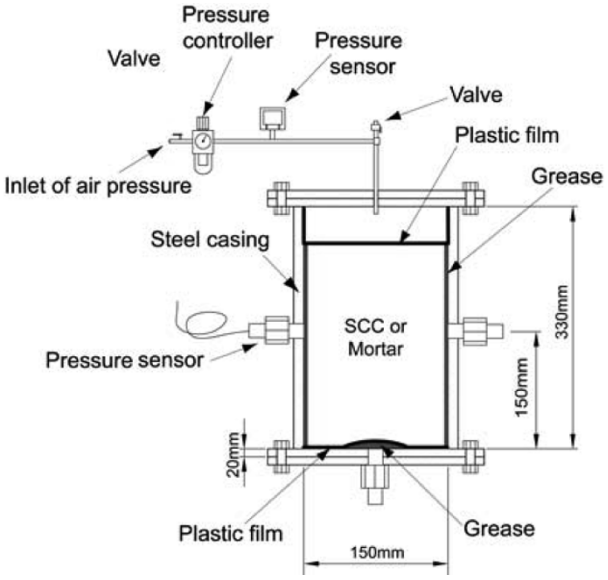

Fig. 4 Test apparatus (redrawn from Kwon et al.[4]).

in Table 1.

Two different cases of loading were applied to the specimens, as shown in Figure 5: (1) Case S1, the vertical pressure is instantly applied at different time after casting and the pressure is then sustained; and (2) Case S2, stepwise and ramp loading are applied. The parameters for $\beta(t)$ and $\alpha(t,t')$ in Eqs. (1) and (2) were calibrated from the results of the first basic test (Case S1). The lateral pressure for Case S2 was calculated with the pre-calibrated parameters following the calculation method described in Eq. (3), and finally the prediction was compared with the measurement in order to verify the model.

Table 1 Mix proportions for experimental verification of the model.

Materials	CP	OC	SCC
	kg for 1 m^3	kg for 1 m^3	kg for 1 m^3
Water	558	195	218
Cement	1394	450	520
Fly ash	-	-	104
Sand	-	776	784
Gravel	-	960	724
HRWRA	-	2.70	5.20

Figure 6 shows the results of the comparison. The hollow dotted lines are the measured lateral pressures, the solid lines are the calculated lateral pressures, and the dotted lines are the applied vertical pressures. For the three samples, CP, OC, and SCC, the prediction is consistent with the measurement, although there are some small errors in peak point and cancellation time. Therefore, it is feasible to employ the proposed model to predict the lateral pressure for any given time-varying vertical pressure.

2.3 Incorporation of the extrinsic factors

The model needs to take many extrinsic factors into account in predicting the real formwork pressure. The friction effect at the interface between the formwork and inner concrete was investigated as one of the major extrinsic factors.[15]

Two different types of tests were performed for mortar and SCC mixes. One was a column formwork test with circular columns of three different diameters (130, 180 and 280 mm) and the same height (1.7 m). The columns were relatively thin and tall, and hence the wall friction should appreciably affect the measured formwork pressure. The other test was a formwork pressure test performed with the apparatus of Figure 4; this test excludes the friction effect to identify the parameters used in the two functions, $\beta(t)$ and $\alpha(t, t')$. The mix proportions are shown in Table 2.

Figure 7 shows a comparison between the lateral pressures measured in the columns and the apparatus, namely, with and without friction conditions. The peak pressure of the column is slightly lower than that of the apparatus, but the difference between the pressures measured in friction and non-friction condi-

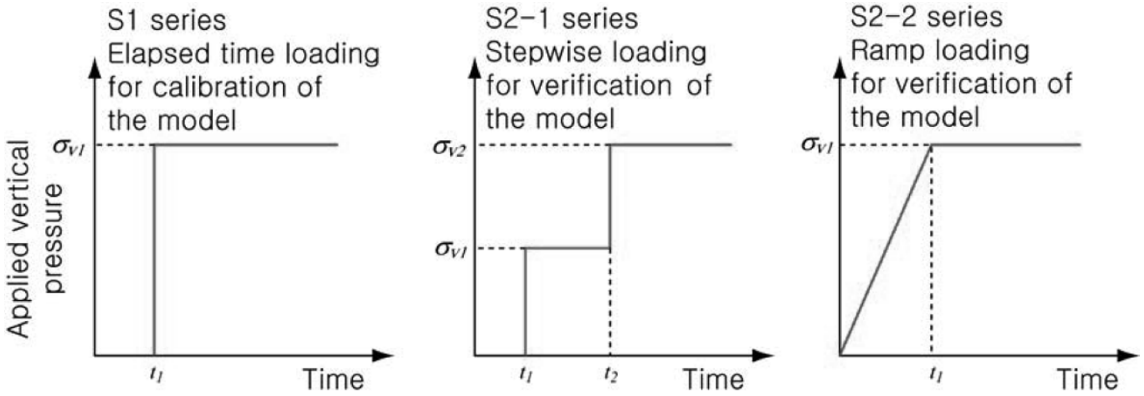

Fig. 5 Applied vertical pressures for calibration and verification of the model (redrawn from Kwon et al.[4]).

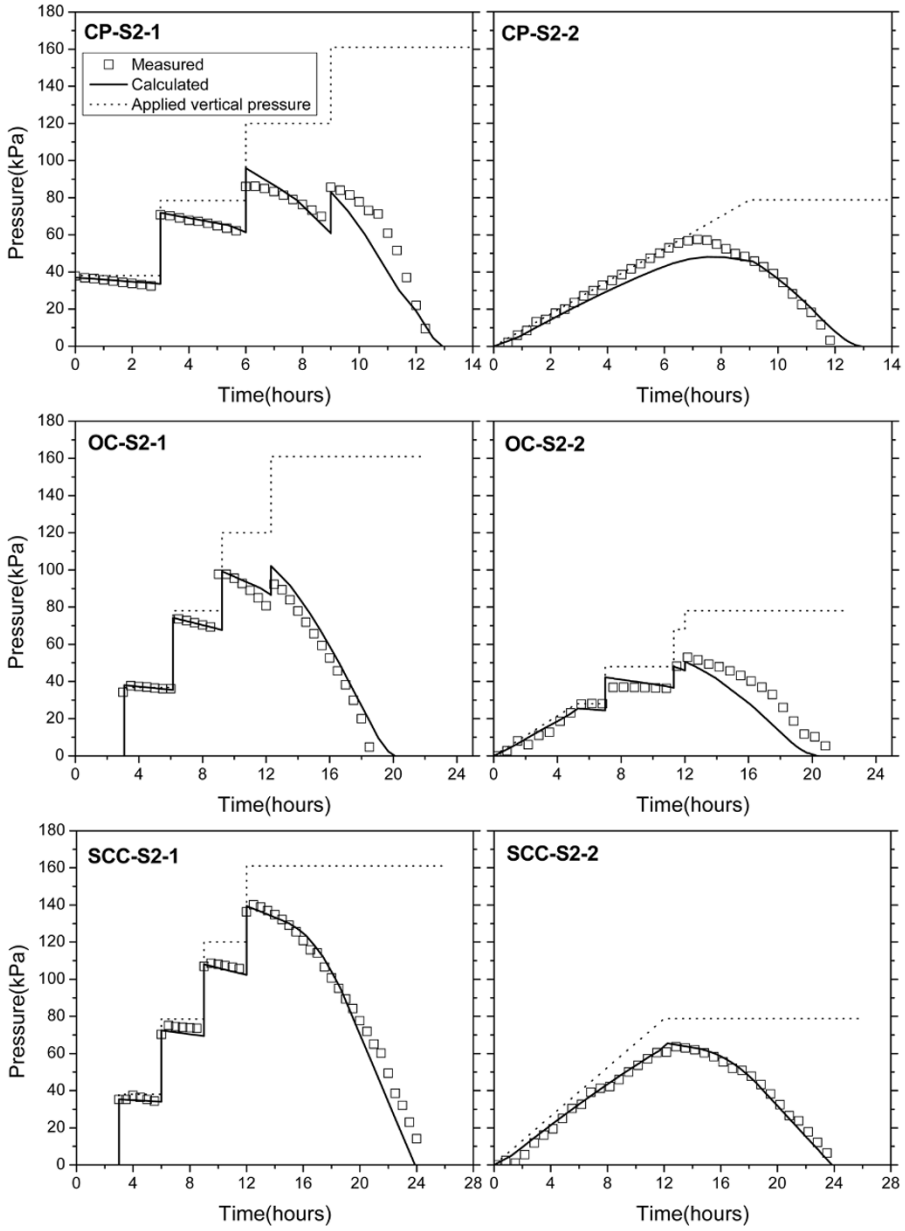

Fig. 6 Measured and calculated lateral pressures for S2 loading series (redrawn from Kwon et al.[4]).

Table 2 Mix proportions for investigation of the effect of wall friction.

Materials	Mortar	SCC
	kg for 1 m^3	kg for 1 m^3
Water	236	182
Cement	479	332
Fly ash	160	111
Sand	1182	819
Gravel	-	875
HRWRA	0.49	1.05
VMA	0.38	1.35

tions increases after the peak. In addition, the cancellation time of the pressure in the columns is considerably earlier than that in the apparatus.

The average friction stress acting on the entire wall surface of the columns was obtained from the pressure measured at the bottom of the columns. The friction stress of the different column diameters was almost identical during casting, but the column with larger diameter had higher friction stress after casting. Figure 8 shows the friction stresses divided by the corresponding diameters. The friction stress-to-diameter ratios are almost identical, with small deviation. The deviation is thought to stem from experimental error. Therefore, it could be concluded that the friction stress is proportional to the column diameter.

The friction stress plays a role of reducing vertical pressure. If the average friction stress τ_{FA} is given, the vertical pressure $\sigma_V(z, t)$ at an arbitrary height z and time t can be expressed by the following equations based on the force equilibrium:

$$\sigma_V(z,t) = \left(w - \frac{P}{A}\tau_{FA}(t)\right) \cdot (h(t) - z) \tag{4}$$

where w is the unit weight of the mixture, A is the cross-section area, and P is the perimeter of the specimen. The mixture height $h(t)$ considers the casting situation. The mixture height increases

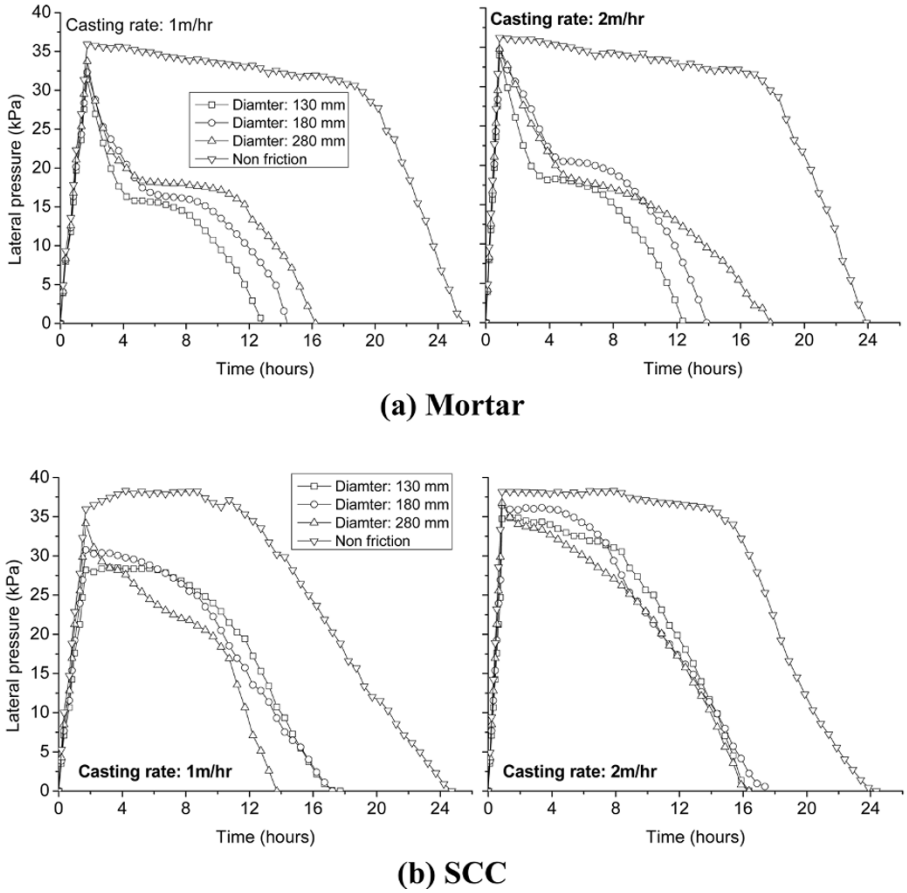

Fig. 7 Measured lateral pressures from the column specimens with friction and the apparatus without friction (redrawn from Kwon et al.[5]).

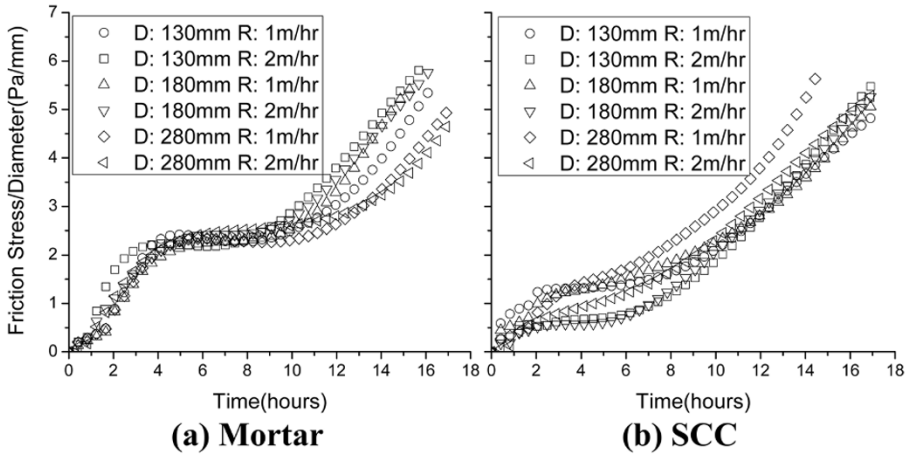

Fig. 8 Values of friction stress divided by the column diameter (redrawn from Kwon et al.[5]).

during casting, and then remains constant as the final height H since the end of placement. The parameters of the two functions, $\beta(t)$ and $\alpha(t, t')$, were calibrated from the small apparatus tests, and the lateral pressures of the columns were calculated by Eqs. (3) and (4). The measured and calculated lateral pressures were compared. Figure 9 shows a comparison for the 280 mm column diameter and 2 m/h casting rate test. Even though there are small differences, both pressures had acceptable agreement, especially for the peak pressure and the cancellation time. As a result, the effect of friction could be quantitatively taken into account in predicting the formwork pressure by incorporating the friction stress into the intrinsic model.

2.4 Application for the peak pressure

The intrinsic model was developed to predict the entire evolution of the formwork pressure, from the beginning of casting until cancellation of the formwork lateral pressure. One of the major concerns is the maximum value of the formwork pressure, for example, when designing a formwork in practice. A simple analytical model that predicts the magnitude of the peak pressure and corresponding lateral pressure profile was suggested based on the intrinsic model.[6]

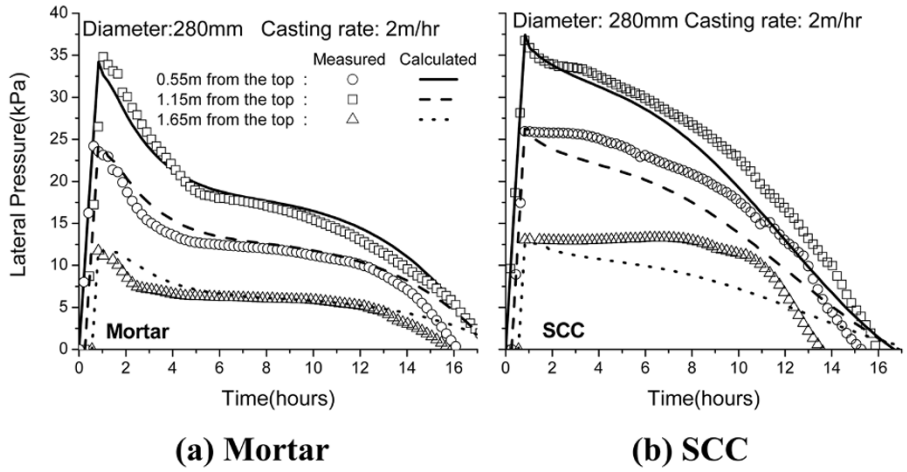

Fig. 9 Comparison between the measured and calculated lateral pressure (redrawn from Kwon et al.[5]).

The two functions $\beta(t)$ and $\alpha(t, t')$ were simplified to consider the time duration of casting:

$$\beta_{simp}(t') = 1 - b \cdot t' \text{ and} \tag{5}$$

$$\alpha_{simp}(t, t') = 1 - a^2 \cdot t' \cdot (t - t') \tag{6}$$

where the parameters a and b are the coefficients representing both functions. The number of parameters was consequently reduced for simplicity.

If a SCC column is filled at a placement rate of R, the vertical pressure increment at the bottom becomes $\Delta\sigma_V(t) = wR \cdot \Delta t$, where w is the unit weight of the SCC mixture. Applying the increment into Eq. (3) gives

$$\sigma_{L,app}(t) = wR\left(t - \frac{b}{2}t^2 - \frac{a^2}{6}t^3 + \frac{ba^2}{12}t^4\right) \tag{7}$$

The 4th-order polynomial function has the maximum value, σ_{max}, at time t_{max}, where t_{max} consequently becomes a function of a and b only. The maximum pressure is calculated by substituting t with t_{max} into Eq. (7):

$$\sigma_{max} = \sigma_{L,app}(t_{max}) = wR \cdot f(a, b) \tag{8}$$

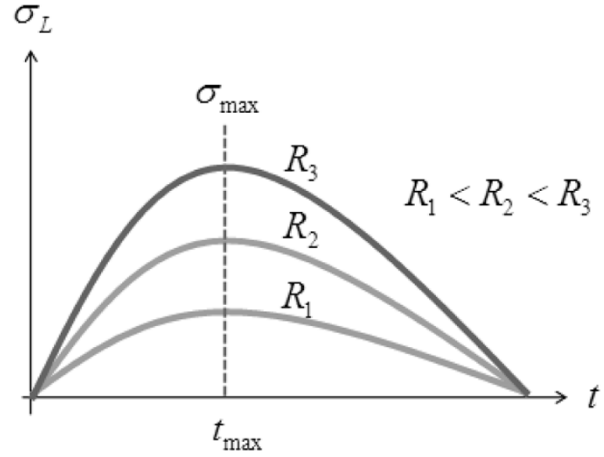

Fig. 10 Maximum lateral pressure for different casting rates (redrawn from Kim et al.[6]).

where $f(a,b)$ is an arbitrary function. Eq. (8) indicates that the maximum formwork pressure is not a function of time but depends on the placement rate and the material properties (namely, the unit weight w and the coefficients a and b). If the same mixture is used for casting, the maximum pressure is proportional to the placement rate, as shown in Figure 10.

In order to find the range of proportion, $f(a,b)$ in Eq. (9), various

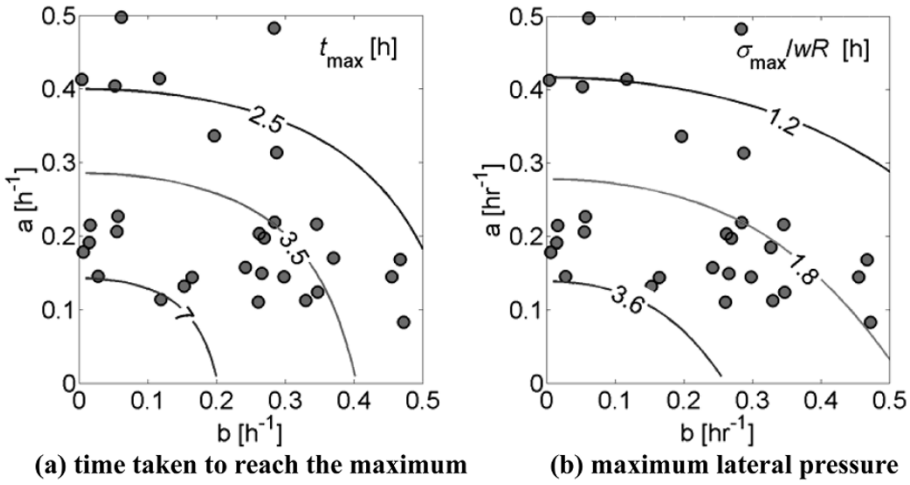

Fig. 11 Range of both coefficients.

Table 3 Mix proportions and measured coefficients.

Label	Composition (kg for 1 m^3) †								Flow (mm)	Results [h^{-1}]	
	W	C	FA	S	G	HRWRA	VMA	Others		b	a
A1	188	362	155	899	798	1.92	2.07	-	672	0.153	0.132
A2	188	362	155	899	798	5.34	2.07	-	655	0.261	0.111
B1	167	386	165	893	792	4.83	2.21	-	679	0.028	0.145
B2	184	362	155	902	799	1.94	2.07	-	648	0.327	0.185
B3	198	341	146	910	807	1.75	1.95	-	736	0.056	0.227
B4	211	322	138	917	813	1.37	1.84	-	800	0.016	0.215
C1	184	362	155	902	799	2.97	2.07	-	616	0.346	0.216
C2	184	362	155	902	800	3.36	2.07	-	591	0.284	0.219
C3	183	362	155	902	800	3.62	2.07	-	686	0.055	0.206
C4	197	359	154	896	795	2.34	1.54	-	705	0.371	0.170
C5	186	362	155	901	799	2.73	-	-	730	0.299	0.145
C6	201	544	-	662	993	3.26	-	-	445	0.288	0.313
C7	201	544	-	662	993	3.81	-	-	600	0.284	0.483
C8	201	544	-	662	993	4.35	-	-	700	0.117	0.415
D1	177	252	151	808	911	6.31	2.02	100	693	0.119	0.114
D2	180	306	153	804	906	4.51	2.04	51.0	660	0.269	0.197
D3	182	333	154	801	904	3.34	2.06	25.6	705	0.266	0.149
E1	182	307	154	904	802	3.67	2.05	51.2	711	0.472	0.083
E2	183	334	154	902	800	2.44	2.06	25.7	622	0.589	0.139
E3	183	351	155	902	800	2.96	2.07	10.3	616	0.262	0.203
E4	183	356	155	901	799	2.97	2.07	5.16	578	0.347	0.124
E5	197	354	154	896	794	2.44	1.54	5.13	660	0.330	0.113
F1	182	356	155	902	800	5.06	2.07	5.16	565	0.242	0.158
F2	184	358	155	901	799	4.64	0.00	3.41	705	0.165	0.144
F3	185	359	155	900	798	3.10	0.00	1.70	597	0.455	0.145
F4	197	358	154	896	794	2.83	1.54	1.69	629	0.467	0.168
G1	201	381	163	662	993	4.35	-	-	720	0.052	0.404
G2	201	326	217	662	993	4.35	-	-	720	0.015	0.191
G3	201	217	326	662	993	3.26	-	-	720	0.197	0.336
H1	201	381	163	662	993	3.81	-	-	720	0.061	0.498
H2	201	326	217	662	993	3.81	-	-	720	0.006	0.179
H3	201	217	326	662	993	3.81	-	-	720	0.004	0.413

†W, C, FA, S, G, HRWRA, and VMA denote water, cement, fly ash, sand, gravel, high-range water-reducing admixture, and viscosity-modifying admixture, respectively. Groups D, E, and F additionally incorporate silica fume, metakaolin clay and attapulgite clay, respectively. The amounts used are listed in the column of Others. In addition, Group G uses limestone powder instead of fly ash.

SCC mixtures were tested, as listed in Table 3. The coefficients a and b were found by the formwork pressure test with a small apparatus similar to that shown in Figure 4.

Figure 11 shows the distribution of the experimental results with the contours of the maximum pressure (σ_{max}) and the time taken to reach the maximum (t_{max}) in Eq. (8). The maximum pressure is normalized with wR, and thus both contours have the unit of hour. The measured coefficients (a and b) for various samples are located on the contour plot. Note that the values of the maximum pressure (σ_{max}) for these experimental data do not exceed $3.6wR$. In other words, the SCC mixtures tested in this study do not exceed the maximum formwork pressure of $3.6wR$.

Figure 12 shows the placement-rate functions for the maximum pressure recommended by ACI[8], DIN[9], and the proposed model: $\sigma_{max} = 3.6wR$, where the unit weight, w, is in the unit of kN/m^3. On the other hand, as shown in Figure 11, the contour corresponding to $\sigma_{max} = 3.6wR$ approximately coincides with that of $t_{max} = 7$ h, indicating that the time needed to reach the maximum pressure $3.6wR$ is about 7 h. However, in many in-field examples, the casting time is clearly less than 7 h, and the peak pressure is expected not to reach $3.6wR$. In those cases, the maximum lateral pressure can be estimated with the time function in Eq. (7) by

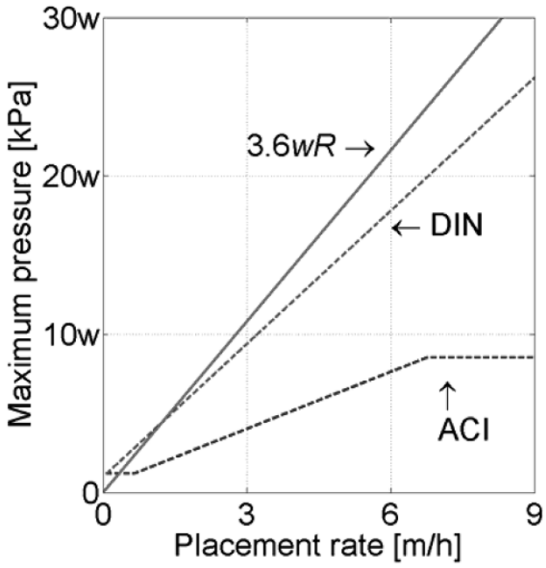

Fig. 12 Placement-rate function for the maximum pressure (redrawn from Kim et al.[6]).

applying the casting time t_{cast} into t. Two general situations were identified: (1) $t_{max} < t_{cast}$: if the casting time is greater than 7 h, the peak pressure would be the placement-rate function, $\sigma_{max} = 3.6wR$. (2) $t_{max} > t_{cast}$: if the casting time is less than 7 h, the peak pressure can be calculated with Eq. (8) by using $t = t_{cast}$.

3. Interpretation based on the model

3.1 Stress state of mixture

Analysis based on the intrinsic model provides considerable insight into the mechanical behavior of SCC fresh mixtures. The mixtures show stiffening due to hydration, capillary suction change, coagulation, floc strength increase, etc., which causes the formwork pressure to decrease over time. The stiffening effect is also identified via rheological measurement, where the yield stress is increasing over time. In some existing studies[11-12], it was assumed that the formwork pressure drop is the same as the amount of yield stress (shear strength) increase over time. However, based on the intrinsic model and experimental observations, the measured shear stress acting on the material during and after casting would not always reach the shear strength or yield stress.

In a cube to which normal stresses are applied, the normal stresses to the x- and y- directions are identical to the lateral pressure σ_L if the normal stress to the z-direction is assigned as the vertical pressure σ_V. The stress state corresponds to the pressure state considered in the model. Figure 13 shows a two-dimensional Mohr circle to represent the stress state of a SCC mixture.

In Figure 13(a), the left graph shows a typical lateral pressure curve over time under a constant vertical pressure, which can be explained by $\alpha(t, t')$ in Eq. (2). State 1 indicates that the lateral and vertical pressures initially are almost the same, and State 3 is the cancellation point of the lateral pressure. As can be seen in the right of Figure 13(a), State 1 corresponds to a point in the Mohr circle, close to the hydrostatic state. The Mohr circle of State 2 becomes larger, toward the left, while the lateral pressure decreases. As the circle grows, the shear stress increases over time. At the end, the left end of the circle reaches the origin when the lateral pressure is cancelled.

The two-function model is further explored in Figure 13(b). While the SCC mixture is under stepwise loading of vertical pressure, the measured lateral pressure can be simulated with $\beta(t)$ and

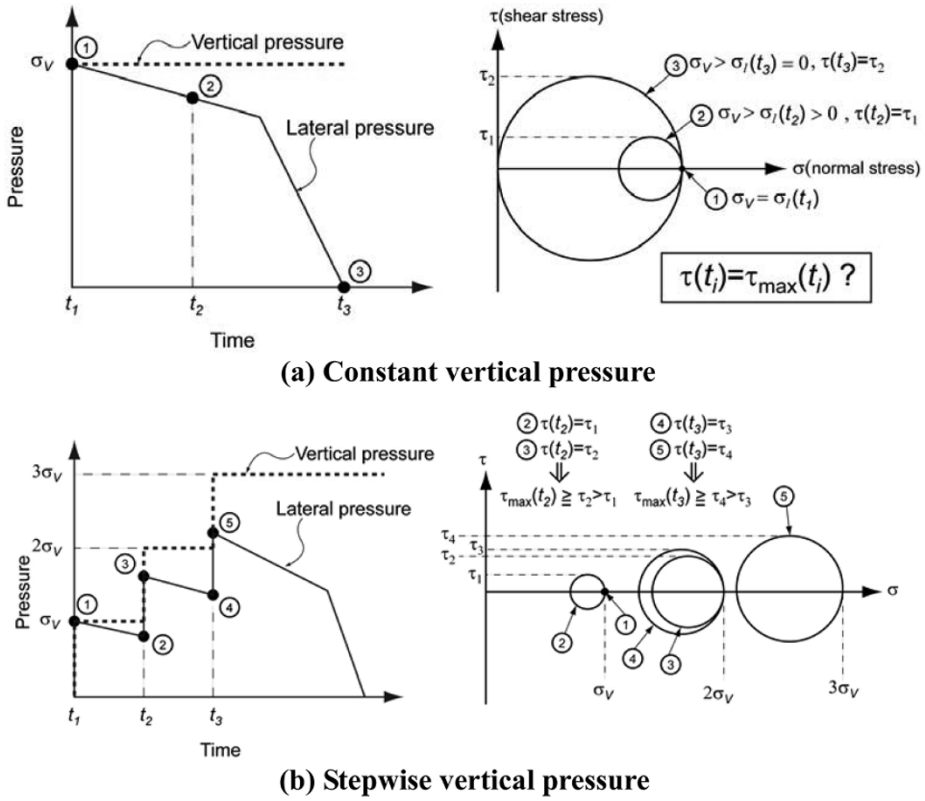

Fig. 13 Difference between shear stress and yield stress.

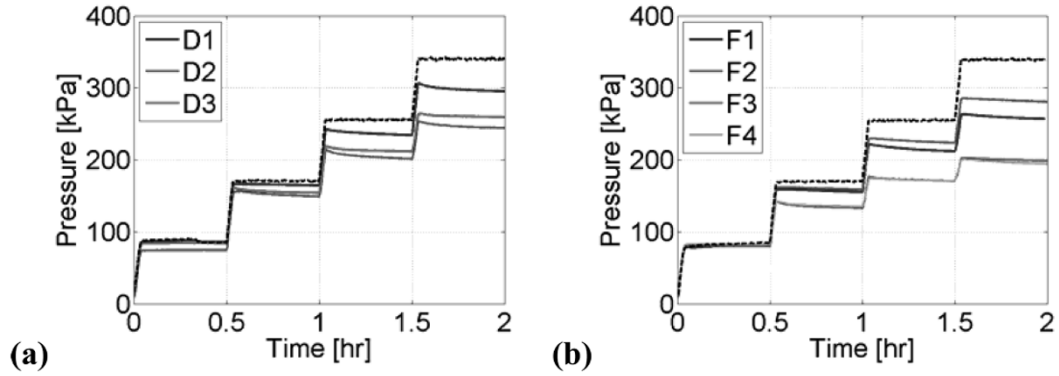

Fig. 14 Effect of mineral admixtures: (a) silica fume and (b) attapulgite clay.

$\alpha(t, t')$. State 1 at $t = t_1$ is modeled with an instantaneous response: $\sigma_L(t_1) = \beta(t_1)\sigma_V(t_1)$. Incorporating a delayed response describes State 2 at $t = t_2$: $\sigma_L(t_2) = \alpha(t_2, t_1)\beta(t_1)\sigma_V(t_1)$. In the same manner, States 3 to 5 can be represented with Eq. (3). On the other hand, Mohr circles represented in the right of Figure 13(b) correspond to each pressure state. It is necessary to take a look at States 2 vs. 3 at $t = t_2$ and States 4 vs. 5 at $t = t_3$. The Mohr circles for States 2 and 3 indicate that the shear stresses acting on a material are different even at the same time ($t = t_2$): the shear stress (τ_1) in State 2 is less than the shear stress (τ_2) in State 3. This indicates that the shear stress at t_1 must be less than the shear strength. The same applies for States 4 and 5 at the same time ($t = t_3$): $\tau_3 < \tau_4 \leq \tau_y$. The stepwise loading measurement perhaps shows that the magnitude of shear stress acting on a fresh concrete mixture is not always the same as its shear strength.

The intrinsic model separately considers the instantaneous shear stress increase for a vertical pressure increment, $\beta(t)$, and the delayed shear stress gain under a constant increment, $\alpha(t, t')$. Despite that the model is phenomenological, it has the merit of predicting realistic formwork pressure without any difficulty related to yield stress. An exact mechanism for the two-function concept has not been clearly revealed yet, but the intrinsic model provides a plausible means of understanding the pressure response of a SCC mixture. The concept also proved helpful to investigate the effects of mineral admixtures, as presented in the following section.

3.2 Effect of mineral admixtures

Incorporation of mineral admixtures affects the formwork pressure of SCC, and the formwork pressure response was investigated based on the proposed model.[7] In the foregoing Table 3, Groups D, E, and F are SCC mixtures containing silica fume (SF), metakaolin clay (MK), and attapulgite clay (AG), respectively. Those groups used the same mix compositions, such as water-cementitious materials ratio, but the HRWRA dosage was adjusted to maintain the slump flow of SCC within a narrow range.

Figure 14 shows the results of the formwork pressure test, where the dashed line is the applied stepwise vertical pressure. The stepwise loading clarified the pressure response in terms of the instantaneous function $\beta(t)$ and delayed function $\alpha(t, t')$. Decreasing slopes of each step are very similar in all cases, which indicates that $\alpha(t, t')$ is not sensitive to the use of mineral admixtures. Table 3 quantitatively reports the observations with the delayed coefficients a distributed within a narrow range. However, the heights of each step, the lateral pressure increments, are appreciably influenced. The measurement was analyzed via $\beta(t)$ and the instantaneous coefficients b are listed in Table 3.

A thixotropic view distinguishes the instantaneous response $\beta(t)$ under sudden increase of pressure from the delayed response $\alpha(t, t')$ under sustained constant pressure. The experimental results show that the instantaneous response is more influenced by the mix proportion. In other words, the microstructure of the mixture customized by incorporating mineral admixtures is more revealed by the mixture test under increasing pressure rather than by that under sustained constant pressure.

Similarly, in a rheological measurement, a SCC mixture under shearing shows different behavior from the identical mixture at rest. By analogy to the instantaneous response $\beta(t)$, a mixture test under shearing is expected to reveal the effects of mineral admixtures effectively. Relating the rheological investigation with the formwork pressure is still questionable and under investigation. Nevertheless, in order to provide a field-friendly test for formwork pressure estimation, a correlation between rheological and formwork pressure tests was identified.[7] The foregoing discussion explicates the reason for selecting the instantaneous response $\beta(t)$ and the loss of slump flow. A slump flow test[12] was also performed in concert with the formwork pressure test for more than 20 mixes. As a result, if the slump flow $d_f(t)$ at time t is measured with the unit of centimeter, the instantaneous function can be estimated:

$$\beta(t) = 0.10 d_f(t) + 0.31 \tag{9}$$

4. Conclusions

This paper summarized the two-function model simulating formwork pressure exerted by SCC. The proposed model uses the instantaneous and delayed response functions separately, which enables consideration of various field conditions such as placement rate and casting procedure. The model shows promise to simulate all situations, but incorporating extrinsic factors and exploring the basic mechanism are still necessary. One of the extrinsic factors, friction between the mixture and formwork, demonstrated in this paper would be an example for future development. The results show that the peak pressure is less influenced by friction, and so the simplified intrinsic model without considering the friction effect is eligible to evaluate the peak pressure of SCC formwork. Based on the SCC formwork pressure test data-

base collected via the studies, the peak pressure is always less than 3.6wR when the casting time is more than 7 hr. If the casting time is less than that, the peak pressure could be further decreased. The value of the decreased peak pressure could be estimated using the loss of slump flow.

Acknowledgements

The authors wish to specially thank Mark Beacraft of Lehigh University, Bethlehem, PA, Noemi Nagy of Budapesti university of Technology and Economics, Hungary, and Quoc Tri Phung of Danang University of Technology, Vietnam, for the collaborative conduct of the formwork pressure test.

References

1. Okamura, H. and Ouchi, M. "Self-compacting concrete, development, present use and future". *Proceedings of the 1st International RILEM Symposium on Self-Compacting Concrete*, Stockholm, Sweden, 1999, pp. 3~14.

2. ACI Committee 237, *Self-Consolidating Concrete*, ACI 237R-07, American Concrete Institute, 2007.

3. Gregori, A., Ferron, R., Sun, Z., and Shah, S. P., "Experimental simulation of self-consolidating concrete formwork pressure," *ACI Materials Journal*, Vol. 105, No. 1, 2008, pp. 97~104.

4. Kwon, S. H., Shah, S. P., Phung, Q. T., Kim, J. H., and Lee Y., "Intrinsic model to predict formwork pressure," *ACI Materials Journal*, Vol. 107, No. 1, 2010, pp. 20~26.

5. Kwon, S. H., Phung, Q. T., Park, H. Y., Kim, J. H., and Shah, S. P., "Effect of wall friction on variation of formwork pressure over time in self-consolidating concrete", *Cement and Concrete Research*, Vol. 41, 2011, pp. 90~101.

6. Kim, J. H., Beacraft, M., Kwon, S. H., and Shah, S. P., "Simple analytical model for formwork design of self-consolidating concrete", *ACI Materials Journal*, Vol. 108, No. 1, 2011, pp. 38~45.

7. Kim, J. H., Beacraft, M., and Shah, S. P., "Effect of mineral admixtures on formwork pressure of self-consolidating concrete", *Cement & Concrete Composites*, Vol. 32, 2010, pp. 665~671.

8. ACI Committee 347, *Guide to Formwork for Concrete*, ACI 347-01, American Concrete Institute, 2001.

9. DIN 18218:2010-01, *Frischbetondruck auf lotrechte Schalungen*, (Pressure of Fresh Concrete on Vertical Formwork), Entwurf, Germany, 2010.

10. Ovarlez, G. and Roussel, N. "A Physical Model for the Prediction of Lateral Stress Exerted by Self-Compacting Concrete on Formwork", *Cement and Concrete Research*, Vol. 39, No. 2, 2006, pp. 269~279.

11. Beitzel, M., Beitzel, H., and Muller, H. S., "Fresh concrete pressure of self-compacting concrete on a vertical formwork," *Proceedings of the Third North American Conference on the Design and Use of Self-Consolidating Concrete*, Edited by Shah, S. P., Chicago, 2008.

12. ASTM C 1611-05, *Standard Test Method for Slump Flow of Self-Consolidating Concrete*, American Society for Testing and Materials, 2005.